

PyQCAMS: Python Quasi-Classical Atom-Molecule Scattering

Rian Koots^{a,b}, Jesús Pérez-Ríos^{a,b,*}

^a*Department of Physics, Stony Brook University, Stony Brook, New York 11794, USA*

^b*Institute for Advanced Computational Science, Stony Brook University, Stony Brook, New York 11794, USA*

Abstract

We present Python Quasi-classical atom-molecule scattering (PyQCAMS), a new Python package for atom-molecule scattering within the quasi-classical trajectory approach. The input consists of mass, collision energy, impact parameter, and pair-wise interactions to choose between Buckingham, generalized Lennard-Jones, and Morse potentials. As the output, the code provides the vibrational quenching, dissociation, and reactive cross sections along with the rovibrational energy distribution of the reaction products. Furthermore, we treat $\text{H}_2 + \text{Ca} \rightarrow \text{CaH} + \text{H}$ reactions as a prototypical example to illustrate the properties and performance of the software. Finally, we study the parallelization performance of the code by looking into the time per trajectory as a function of the number of CPUs used.

Keywords: Atom-molecule scattering; quasi-classical trajectory calculations; molecular dissociation; vibrational quenching; reactive scattering.

PROGRAM SUMMARY

Program Title: PyQCAMS: Python Quasi-Classical Atom-Molecule Scattering

CPC Library link to program files: (to be added by Technical Editor)

Developer's repository link: <https://github.com/Rkoost/PyQCAMS>

Code Ocean capsule: (to be added by Technical Editor)

Licensing provisions: MIT

*Corresponding author.

E-mail address: jesus.perezrios@stonybrook.edu

Preprint submitted to Computer Physics Communications

April 7, 2023

Programming language: Python

Nature of problem: Simulation of atom-molecule scattering systems.

Solution method: Quasi-Classical trajectory method and numerical solution of Hamilton's equations.

1. Introduction

For decades, one of the main approaches to studying molecular dynamics has been via the quasi-classical trajectory (QCT) method [1, 2]. This technique treats collisions semi-classically. The nuclear dynamics in the underlying potential energy surface is treated classically. However, the initial and final states are picked following the Bohr-Sommerfeld quantization rule, yielding accurate predictions at significantly less cost than quantum dynamics as long as they fall within given conditions regarding the collision energy –number of contributing partial waves [3, 4]. QCT has been used in multitude of scenarios relevant to chemical physics [5, 6, 7, 8, 9, 10, 11], and cold and ultracold chemistry [12, 13, 14], ranging from the ultracold to the hyperthermal regimes. In particular, It has been used to study the relaxation and reaction dynamics of cold atom-ionic molecule [13, 12] and atom-molecule collisions [15].

We present an open-source, object-oriented program written in Python to perform QCT calculations on atom-molecule systems called Python Quasi-Classical Atom-Molecule Scattering (PyQCAMS). While chemical dynamics programs such as Gaussian [16] and VENUS [17], we introduce a more accessible, user-friendly and dedicated path to performing these simulations. Our program consists of completely open-source software, and relies mainly on the NumPy [18] and SciPy [19] packages. We use matplotlib[20] for data visualization, pandas[21] for data storage and analysis, and multiprocessing [22, 23] for parallel implementation.

The outline of this paper is as follows: In Section 2 we discuss the theory behind the quasi-classical trajectories method, including initial conditions, trajectory reactions, and analysis. In Section 3, we discuss the PyQCAMS program as separated into the inputs, main code, and outputs. We also discuss the implementation and performance of the program. In Section 4, we provide an example of a typical workflow to study the reaction ($\text{H}_2 +$

Ca), where we outline how a user can obtain reaction rates and product distributions using the program.

2. Theoretical approach

In this section we describe the basics of QCT. The quasi-classical trajectory (QCT) method treats scattering processes semi-classically. First, by solving Newton’s equations of motion of the colliding nuclei. Next, in the case of atom-molecule scattering, at the start of each trajectory, the internal degrees of freedom of the molecule are treated within the Wentzel-Kramers-Brillouin (WKB) approximation, such that the initial rovibrational state (v, j) satisfies a quantum-mechanically viable state. The classical Hamiltonian for a 3-particle, atom-molecule system with masses m_i , $i = 1, 2, 3$ takes the form:

$$H = \sum_{i=1}^3 \frac{\vec{p}_i^2}{2m_i} + V(\vec{r}_1, \vec{r}_2, \vec{r}_3) \quad (1)$$

where \vec{p}_i and \vec{r}_i represent the momentum and position vectors of each atom with respect to the origin. This Hamiltonian is expressed in Jacobi coordinates as:

$$H = \frac{\vec{P}_1^2}{2\mu_{12}} + \frac{\vec{P}_2^2}{2\mu_{123}} + V(\vec{\rho}_1, \vec{\rho}_2) \quad (2)$$

where $\vec{\rho}_1$ is the Jacobi vector associated with the molecule and \vec{P}_1 is its conjugate momentum. $\vec{\rho}_2$ is the Jacobi vector connecting the atom with the center of mass of the molecule, and \vec{P}_2 is its conjugate momentum, as shown in Fig. 1. Note that this Hamiltonian uses the reduced masses of the corresponding atoms: $\mu_{12} = (\frac{1}{m_1} + \frac{1}{m_2})^{-1}$ and $\mu_{123} = (\frac{1}{m_3} + \frac{1}{m_1+m_2})^{-1}$. Defining the coordinates in this way separates the center-of-mass degree of freedom from the relative one. Then, the momentum associated with the center-of-mass degrees of freedom is a constant of motion since the interaction potential do not depend on the center-of-mass position, and neglected in the analysis of the dynamics..

We trace the atoms’ subsequent motion by solving Hamilton’s equations of motion:

$$\frac{d\rho_{i,\alpha}}{dt} = \frac{\partial H}{\partial P_{i,\alpha}} \quad (3)$$

$$\frac{dP_{i,\alpha}}{dt} = -\frac{\partial H}{\partial \rho_{i,\alpha}} \quad (4)$$

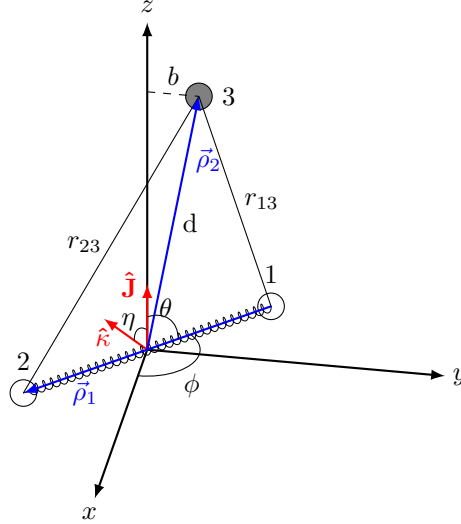


Figure 1: (Color online.) Jacobi coordinates of a atom-molecule system. Here, the molecule is rotating in the x-y plane, with the angular momentum \vec{J} along the z-axis and $\vec{\kappa} = \vec{\rho}_1 \times \hat{z}$. η is the angle between $\vec{\kappa}$ and \vec{J} , and ϕ and θ are defined as usual in spherical coordinates.

for $i = 1, 2$ for each associated vector and $\alpha = 1, 2, 3$ for each Cartesian component.

2.1. Initial Conditions

The initial orientation angles are randomly generated to initialize each trajectory. The momentum of the molecule, \vec{P}_1 , is subsequently defined by the orientation angles. If we initialize the molecule at its classical outer turning point $|\vec{\rho}_1| = r_+$, the momentum has no radial component. Since the angular momentum $\vec{J} = \vec{r} \times \vec{p}$, and the fact that $\vec{\rho}_1 \perp \vec{P}_1$, we find the magnitude of $P_1 = \hbar\sqrt{j(j+1)}/r_+$, with components [4]:

$$\vec{P}_1 = P_1 \begin{pmatrix} \sin \phi \cos \eta - \cos \theta \cos \phi \sin \eta \\ -\cos \phi \cos \eta - \cos \theta \sin \phi \sin \eta \\ \sin \theta \sin \eta \end{pmatrix} \quad (5)$$

The initial vibrational phase is randomly generated by choosing the initial distance between the atom and molecule as

$$R = R_0 + \frac{\chi P_2 \tau_{v,j}}{\mu_{123}} \quad (6)$$

where R_0 is a fixed far-away distance where the interaction potential strength is negligible. The second term probes the molecule's vibrational phase since $\chi \in [0, 1]$ is randomly generated following a uniform distribution and $\tau_{v,j}$ is the vibrational period of the molecule corresponding to the quantum-mechanical state (v, j) . This is calculated as

$$\tau_{v,j} = \sqrt{2\mu_{12}} \int_{r_-}^{r_+} \left[E_{int} - V(r_{12}) - \frac{\hbar^2 j(j+1)}{2\mu_{12}r_{12}^2} \right]^{-\frac{1}{2}} dr \quad (7)$$

where $V(r_{12})$ is the molecular potential energy and r_{12} is the molecular separation. E_{int} is the internal energy of the molecule, which is calculated following a discrete variable representation (DVR) method using particle-in-a-box eigenfunctions [24].

2.2. Reaction Products

For the atom-molecule reaction $AB + C$, we expect three possible final products:

1. Inelastic collision (quenching): $AB(v) + C \rightarrow AB(v') + C$
2. Molecular formation (reaction): $AB + C \rightarrow AC + B$ or $BC + A$
3. Dissociation: $AB + C \rightarrow A + B + C$

The final product is determined by the relative energy between each atom. The condition for whether two atoms are bound is determined by the effective potential:

$$E_{ab} < \begin{cases} V_{ab}(r_0) + \frac{j'(j'+1)}{2\mu_{ab}r_0^2} & j' \neq 0 \\ 0 & j' = 0 \end{cases} \quad (8)$$

where r_0 is the local maximum of the effective potential. Here, $a, b \in [1, 3]$ represent each of the atoms. Two atoms are considered bound only if this condition is satisfied for just one pair of atoms, so that the other two pairs can be deemed unbound.

In the same manner as the initial rovibrational states (v, j) , the final states (v', j') are calculated within the WKB approximation. The rotational quantum number is given by:

$$j' = -\frac{1}{2} + \frac{1}{2} \sqrt{1 + 4 \frac{\vec{J}' \cdot \vec{J}'}{\hbar^2}} \quad (9)$$

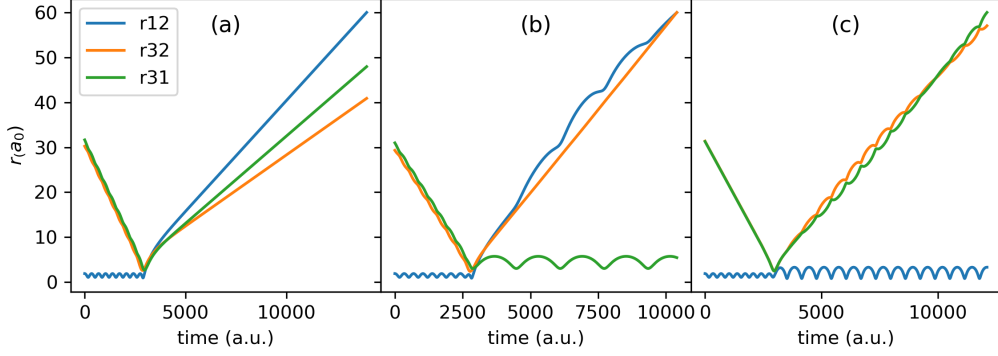


Figure 2: (Color online.) Different product outcomes for a given QCT calculation for $\text{H}_2 + \text{CaH}$ at $E_c = 50000$ K, $b = 0$ a_0 . r_{12} represents the internuclear distance between each H, whereas r_{32} and r_{31} represent the internuclear distance between the colliding atom Ca (3) and each molecular atom (H(1) and H(2)). These trajectories show dissociation (a), reaction (b), and quenching (c). In panel (b), r_{31} oscillates around a fixed distance, an indicator that a new molecule is formed.

where $\vec{J} = \vec{\rho}_i \times \vec{P}_i$ is the effective conjugate angular momentum of the Jacobi vector $\vec{\rho}_i$. The vibrational quantum number is given by:

$$v' = -\frac{1}{2} + \frac{\sqrt{2\mu_{ab}}}{\pi\hbar} \int_{r_-}^{r_+} \left[E'_{int} - V(r_{ab}) - \frac{\hbar^2 j'(j'+1)}{2\mu_{ab}r_{ab}^2} \right]^{\frac{1}{2}} dr \quad (10)$$

Although these equations lead to continuous numbers, they need to be interpreted as integers before assigning them as quantum numbers. This is done through the Gaussian binning (GB) process, where each v' is weighted against its nearest integer v_t with a Gaussian [3]:

$$W_{q,r}(v', v_t) = \frac{1}{\sigma\sqrt{2\pi}} e^{-\frac{|v'-v_t|^2}{2\sigma^2}} \quad (11)$$

2.3. Analysis

The cross section and reaction rates for an atom-molecule collision are calculated from QCT simulations. The first step in doing so is to calculate the opacity function, which is formally defined as

$$P_{q,r,d}(E_c, b) = \int P_{q,r,d}(E_c, b, \theta, \phi, \eta, \chi) d\Omega \quad (12)$$

where $d\Omega = \sin\theta d\theta d\phi d\eta d\chi$. This integral is evaluated via the Monte Carlo technique over the randomly generated variables θ, ϕ, η , and χ .

$$P_{q,r,d}(E_c, b) = \frac{N_{q,r,d}(E_c, b)}{N} \pm \delta_{q,r,d}(E_c, b) \quad (13)$$

The final state distribution of, for example, a reaction is calculated via the Gaussian Binning method [25]:

$$P_r(E_c, b, v_t) = \frac{\sum_{i=1}^{N_r} W_r^i(v', v_t)}{W} \quad (14)$$

with the total weight W evaluated as

$$W = \sum_{v_t} \left(\sum_i^{N_r} W_r^i(v', v_t) + \sum_i^{N_q} W_q^i(v', v_t) \right) + N_d \quad (15)$$

where N_r, N_q , and N_d are the number of reaction, quenching, and dissociation products, respectively. Each Gaussian weight is summed over both the total number of products and the total number of vibrational states produced by the scattering process. Each dissociation reaction has a weight $W_d = 1$ since there is no vibrational state associated with this product.

For N calculations, the opacity function $P_{q,r,d}(E_c, b)$ gives the probability of quenching (q), reacting (r), or dissociation (d) and δ is the error associated with the Monte Carlo technique:

$$\delta_{q,r,d} = \frac{\sqrt{N_{q,r,d}(E_c, b)}}{N} \sqrt{\frac{N - N_{q,r,d}(E_c, b)}{N}} \quad (16)$$

3. The program

PyQCAMS is written in an object-oriented manner, containing three main classes; `Potentials`, `Energy`, and `QCT`. This allows for the addition of new methods within each step of the calculation outlined in Figure 3. The program takes an input file where the user specifies the details of the reaction of interest. The variables are passed into their respective classes, where the trajectory calculations are performed. The results of each trajectory are then output into a `csv` file. The details of each step are outlined in this section.

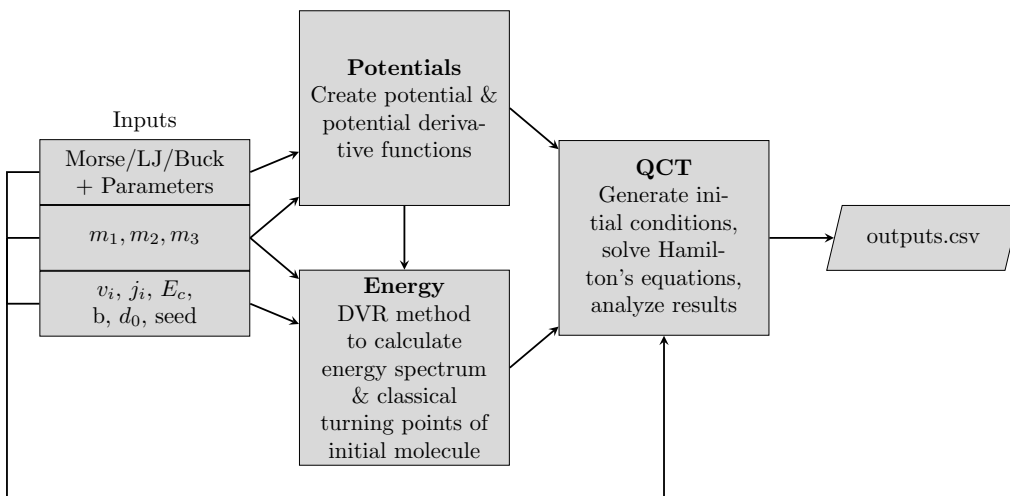


Figure 3: The general structure of the PyQCAMS program.

3.1. Input

The input file is a JSON file whose keywords are described in this section (Listing 1). Each trajectory is tuned by the initial rovibrational energy level of the molecule v_i , j_i , the collision energy E_c (K), impact parameter b , and initial distance between the atom and molecule r_0 . For reproducibility, the user can input a `seed` for the random number generator, or leave it as null to generate a new random number. The interaction potential between each atom is also tune-able, with choices from the Morse, generalized Lennard-Jones, and Buckingham potentials. The user should choose each of these internuclear potentials labeled as “potential_AB (BC,CA)”. Note that AB should always represent the initial molecule, so that the “C” represents the colliding atom. This convention should also be followed when specifying the masses.

The associated parameters of each of these potentials must be entered by the user, which are outlined in Section 3.2. Since the energy spectrum is calculated via the DVR method, the user should also enter the number of DVR points and specify the range for which the potential is well-defined, such that it captures the potential minimum, short-range, and long-range behavior.

Finally, the parameters for integration should be entered. The user can choose when to stop a trajectory using `t_stop`, which is a multiplicative factor of the trajectory’s time scale. Another stopping condition is the maximum

distance between any two atoms, `r_stop`. Finally, the absolute and relative tolerances of the integrator can be controlled with `a_tol`, `r_tol`.

Note that all values entered in the input file should be in atomic units except for collision energy, which is in K for the user's convenience. However, when importing the energy into the program, ensure that it is converted to atomic units, as is done in the `start()` method.

```

1  {"vi": 0,
2  "ji": 0,
3  "Ec (K)": 30000,
4  "b": 0,
5  "r0": 30,
6  "seed": null,
7  "potential_AB": "morse",
8  "potential_BC": "morse",
9  "potential_CA": "morse",
10 "masses":{"ma": 1837.47165336,
11           "mb": 1837.47165336,
12           "mc": 73046.7897752},
13 "int_params":{"t_stop": 15,
14               "r_stop": 60,
15               "a_tol": 1E-10,
16               "r_tol": 1E-11},
17 "potential_params":{"
18   "AB":{"npts": 1000,
19         "xmin": 0.5,
20         "xmax": 10,
21         "morse":{"re" : 1.40104284795,
22                 "de"  : 0.16456603489,
23                 "we"  : 0.02005340207},
24         "lj":{"m":6,
25              "n":12,
26              "re" : 1.40104284795,
27              "cm": 6.49902670540583931313,
28              "cn": 64.16474114146757},
29         "buck":{"a": 167205.03207304262,
30                "b": 8.494089813101883,
31                "c6": 6.49902670540583931313,
32                "re" : 1.40104284795,
33                "max": 0.2}
34   },
35   "BC": { ... },
36   "CA": { ... }
37 }
```

Listing 1: The input file for an $\text{H}_2 + \text{CaH}$ trajectory calculation. Each parameter is explained in the text. The potential parameters for molecules BC and CA are collapsed to save space, but contain the same variables as those for AB.

3.2. Main Code

The `Potentials` class houses the interaction potentials. Each method in this class represents a different potential, and returns a tuple of two function objects: the potential and its derivative. This class is useful for studying and manipulating the effect of different potentials on different pairs of the atom-molecule system. Results can be sensitive to the chosen potential, so it is important to test different potentials when studying a system. The available potentials and associated parameters are:

1. Morse: $V(r) = D_e (1 - \exp(-\alpha(r-r_e)))^2 - D_e$
Parameters required: D_e, r_e, w_e
2. Generalized Lennard-Jones: $V(r) = C_m/r^m - C_n/r^n$
Parameters required: $m, n, C_m, C_n,$ and r_e (guess left)
3. Buckingham: $V(r) = ae^{-br} - C_6/r^6$
Parameters required: $a, b, C_6,$ and r_e (guess left). “max”: Guess of where the maximum is. At short range, Buckingham potentials can reach a maximum and collapse. Enter your nearest r value to this maximum.

Note that while r_e is not a parameter in the analytical expressions of the generalized Lennard-Jones and Buckingham potentials, it is required as part of a root solver method. The `Energy` class houses the DVR method and turning point calculations. This is a separate class since these quantities should be computed once at the beginning of each trajectory. The spectrum and turning points for different $E_{(v,j)}$ in different potentials can be stored separately for future use.

The `QCT` class performs the main QCT calculation, and is outlined in Figure 4. The `iCond()` method uses the calculated parameters from the `Energy` and `Potentials` class to generate a random set of initial conditions, yielding $(\vec{\rho}_1, \vec{\rho}_2, \vec{P}_1, \vec{P}_1)$. The `hamEq()` function writes the Hamilton’s equations of motion, and serves as an input function to `solve_ivp()`, a SciPy [19] integrator utilizing the adaptive Runge-Kutta 5(4) integration method [26]. The `vPrime()` method serves to calculate Equation 10, yielding the final state vector \vec{s}_f . The integrator is housed in the `run_T()` method, which processes the results and assigns the relevant outputs as attributes of the `QCT` class.

The `hamiltonian()` method defines the Hamiltonian of the system, and outputs the total energy and momentum, useful for checking conserved quantities.

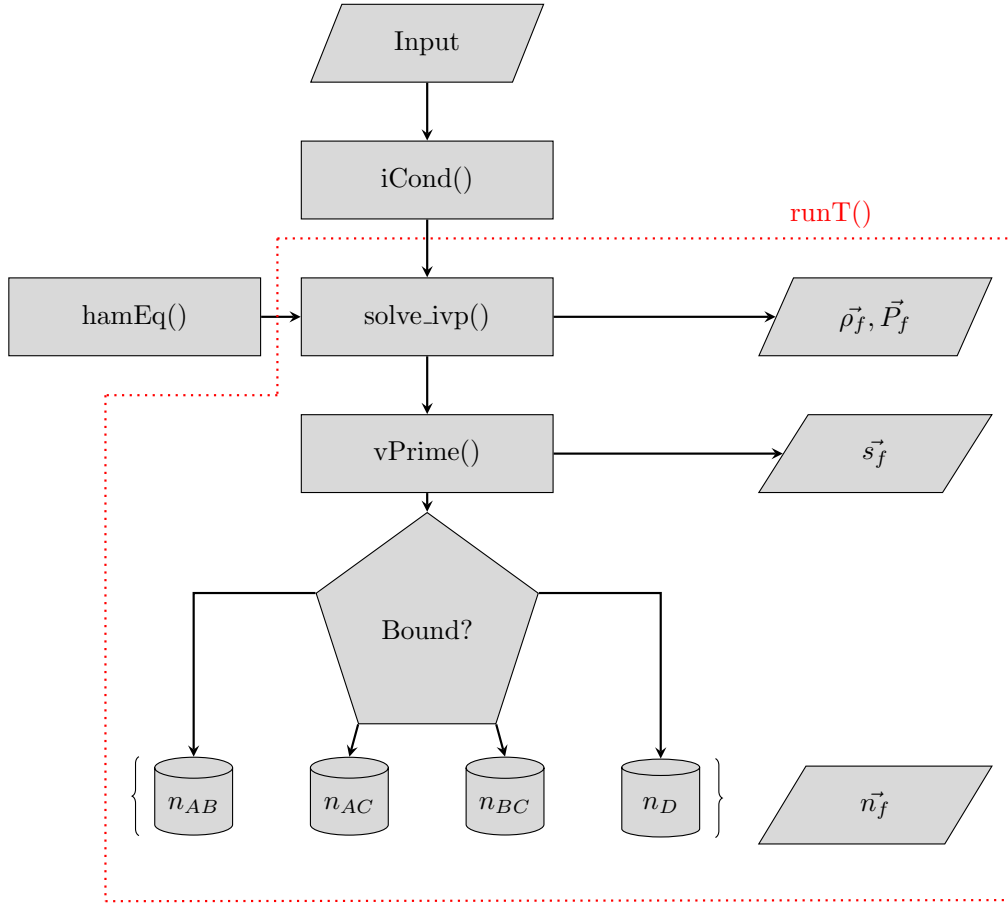


Figure 4: Outline of the QCT class. The components within the dashed line are contained in the `run_T()` method of the QCT class. The outputs are the final position, momentum, state, and product count vectors. The product count vector is defined by the final product bins, filled according to which pair of atoms is bound.

3.3. Output

For a single trajectory, the outputs are:

1. Product count $\vec{n}_f = (n_q, n_{r_1}, n_{r_2}, n_d)$ where $n_{q,r_1,r_2,d}$ is either 0 or 1. For atom-diatomic molecule scattering, the two possible reactions are represented by n_{r_1} and n_{r_2} .
2. Final state $\vec{s}_f = (v_t, w(v', v_t), j)$ where $w(v', v_t)$ is the Gaussian weight given in equation 11. For trajectories yielding $n_d = 1$, the final state outputs $\vec{s}_f = (0,0,0)$.
3. Final positions $\vec{\rho}_f = (\rho_1, \rho_2)$
4. Final momenta $\vec{P}_f = (\vec{P}_1, \vec{P}_2)$
5. Final time t_f

Each trajectory is labeled by the input parameters (E_c, b) .

3.4. Parallel Implementation & Performance

The code is best used in a parallel implementation, which dramatically speeds up the time per trajectory as the number of CPUs is increased (Figure 5). The `save_short()` and `save_long()` methods from `util.py` file uses the Python package `multiprocess` to do this. As shown in the `sim.py` file, the user can choose to save a long output, where the program outputs a new line per trajectory containing all of the output data, or a short output, which creates a new line per (E_c, b) by summing the product count vector \vec{n}_f . The long output is required for final state distribution analysis. Figure 5 shows the time per trajectory as the number of CPUs varies, averaged over 1000 trajectories. This was performed on Stony Brook’s Seawulf cluster. It is clear that parallel processing yields a significant decrease in the total time. The majority of the calculation time is spent during the solution of the Hamilton’s equations of motion. Note that for parallel processing, the `multiprocess` package is required. This package uses `dill`, which gives more flexibility in what can be serialized for parallel computation. The `solve_ivp` API allows the user to control absolute and relative tolerances to control local error estimates. These can be controlled via the input file, and will have a large influence on the energy conservation and time per trajectory. It is highly recommended to study the effect that these tolerances have on a system before running large calculations. Each QCT object has a `delta_e` attribute which yields the total change in energy over the trajectory.

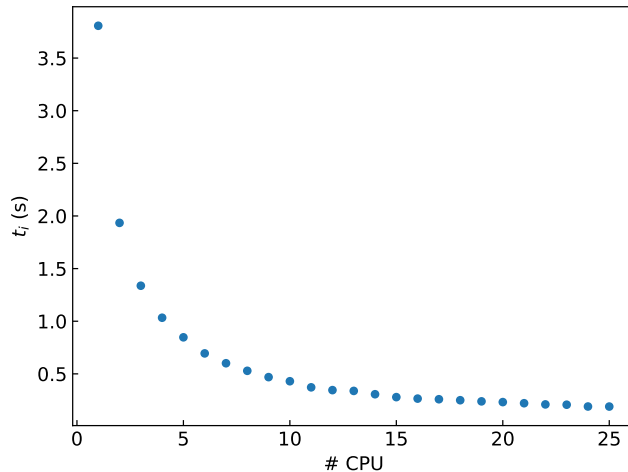


Figure 5: Time per trajectory as a function of the number of CPUs used in the parallel calculation. These trajectories were run at a collision energy of 40000 K for $\text{H}_2 + \text{Ca}$ reactions, with a relative tolerance of 10^{-12} and absolute tolerance of 10^{-11} .

3.5. Visualization

The file `plotters.py` contains several methods for visualizing the results of a trajectory. Fig. 2 was obtained using the `traj_plt` function, which requires a trajectory object as input. There is also a 3d plot generator `traj_3d` which provides a trace of the event. Finally, there is a method to generate an animation of the trajectory, `traj_gif`. The usage of these plotters is shown in the example Jupyter notebook.

4. Example

As an example, we demonstrate the calculation of CaH formation rate as a result of the reaction $\text{H}_2 + \text{Ca} \rightarrow \text{CaH} + \text{H}$. The input file `inputs.json`. All of the simulation and potential parameters are listed. The potential ranges and parameters for H_2 and CaH were obtained from [27, 28] and [29, 30], respectively. We include the parameters of the three potentials we might be interested to study this system in; Morse, Lennard-Jones ('lj'), and Buckingham ('buck'). Here we choose the Morse potential to describe the interaction of both H_2 and CaH:

$$V(r) = D_e \left(1 - \exp(-\alpha(r-r_e))\right)^2 - D_e \quad (17)$$

In this example, we run 10^4 trajectories in parallel, looped over 20 impact parameters. (Listing 2)

```

1 import pyqcams.pymar as pymar
2 import numpy as np
3 import pyqcams.util as utils
4 import os
5
6 if __name__ == '__main__':
7     calc = pymar.start('inputs.json') # Calculated parameters for
8         main function
9
10    n_traj = 10000 # Number of trajectories
11    out_file = f'example/results_short.csv'
12    cpus = os.cpu_count() # Number of cpus for parallel calculation
13    bvals = np.arange(0,5,.25) # Range of impact parameters
14
15    # loop over all impact parameters
16    for b in bvals:
17        calc['b'] = b # set new impact parameter
18        # Uncomment below for long output
19        # utils.save_long(n_traj, cpus, calc, f'{out_file}')
20        # Uncomment below for short output
21        utils.save_short(n_traj, cpus, calc, f'{out_file}')

```

Listing 2: Parallel implementation of PyQCAMS with comments. The “utils.save_short()” runs the quasiclassical trajectories in parallel and outputs the summed data to the specified “out_file”.

The output data now has $\sim 10000 \times 20$ lines, each corresponding to one trajectory. Each of the 20 impact parameters leads to a different opacity function for a reaction, $P_r(E_c, b)$. The opacity function yields the scattering cross section at different collision energies E_c :

$$\sigma_{q,r,d}(E_c) = 8\pi^2 \int_0^{b_{max}^{q,r,d}} P_{q,r,d}(E_c, b) b db \quad (18)$$

and the rate

$$k_{q,r,d}(E_c) = \sigma_{q,r,d}(E_c) \sqrt{\frac{2E_c}{\mu}} \quad (19)$$

For this example, we repeated the code in Listing 2 over 10 different collision energies E_c . For each E_c , we sum over the count vector \vec{n} to obtain the opacity function, cross section, and rate as described. The rates for CaH formation are shown in Figure 6, where it is noticed that higher collision energies gives

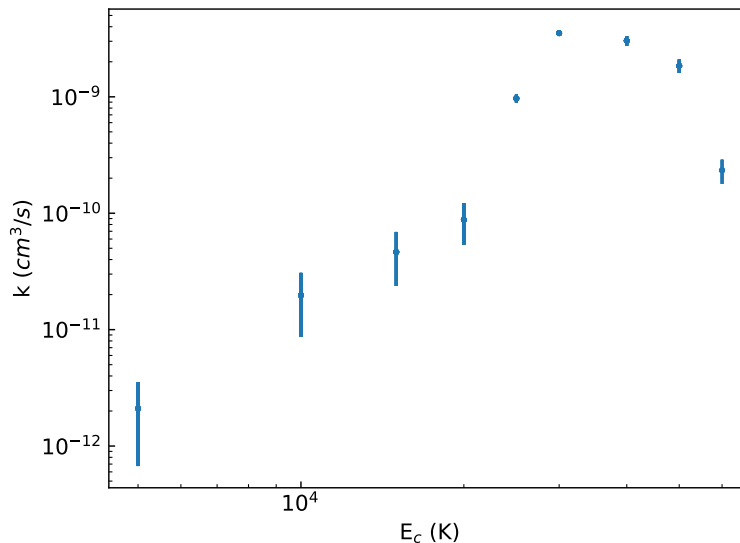


Figure 6: Rate of reaction $\text{H}_2 + \text{Ca} \rightarrow \text{CaH} + \text{H}$. 9 different collision energies were considered, and 10^4 trajectories were run at each energy. We use 20 evenly spaced impact parameters between 0 and $5 a_0$ for each collision energy. Here, the H_2 molecule was initiated at $v = 1$, $j = 0$ and each pairwise interaction was defined by a Morse potential. From here, we see that CaH is most likely formed at a collision energy $E_c = 30000$ K.

rise to larger reaction rates, as expected in endothermic reactions. However, at very high collision energies such a trend changes due to the dominance of molecular dissociation processes. A more detailed study of this reaction will be published elsewhere.

We can also calculate the distribution of states of CaH and H_2 , using the final state vector \vec{s} . Figure 7 shows these distributions at four different collision energies. We can see that the higher vibrational states fill up for both CaH and H_2 as the collision energy is increased, as is typical in endothermic reactions. All details of these calculations can be found in a Jupyter notebook example file.

5. Conclusions

We have presented a Python quasi-classical atom-molecule scattering program, PyQCAMS. The PyQCAMS program aims to provide an easy-to-use platform for calculating quasi-classical trajectories for atom-diatom

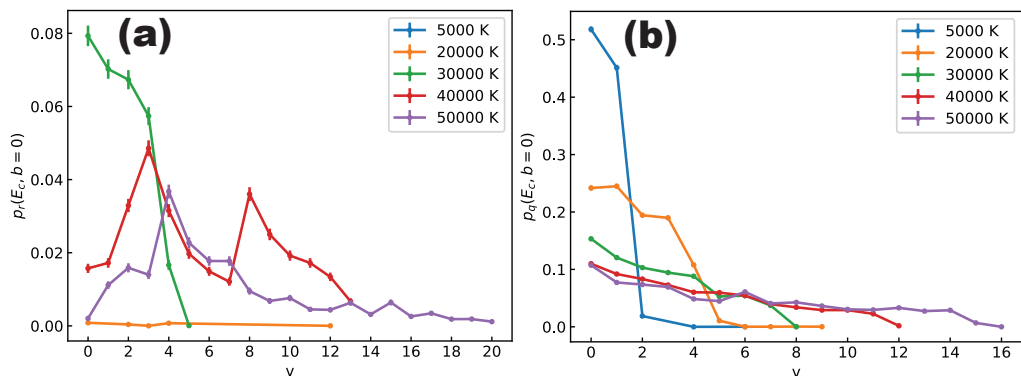


Figure 7: (Color online.) Probability distribution of final vibrational states of CaH (a) and H₂ (b) as a result of the reaction H₂ + Ca, calculated by PyQCAMS. H₂ was initiated at $v = 1$, $j = 0$, with each pairwise interaction defined by a Morse potential. Each color represents a different collision energy E_c , and the impact parameter of each trajectory is fixed to $b = 0$.

molecule systems, including the three most relevant potentials for diatomic molecules: Morse, Buckingham and the generalized Lennard-Jones. We discussed the underlying theory behind the program, and the methods of the program as they pertain to the theory. As output, the user obtains the reaction probability per energy and impact parameter. Then, with this information is possible to calculate the cross section and energy-dependent rate constant. Its object-oriented approach allows the user to study different properties of a given trajectory. The plotter tools make it easy to visualize the results of a trajectory, making it ideal for a new researcher studying trajectories or for presenting the topic in a classroom setting.

6. Acknowledgments

The authors acknowledge the generous support of the Simons Foundation.

References

- [1] M. Karplus, R. N. Porter, R. D. Sharma, Exchange reactions with activation energy. i. simple barrier potential for (h, h₂), *The Journal of Chemical Physics* 43 (9) (1965) 3259–3287. arXiv:<https://doi.org/10.1063/1.1697301>, doi:10.1063/1.1697301. URL <https://doi.org/10.1063/1.1697301>

- [2] D. G. Truhlar, J. T. Muckerman, in: Atom-molecule collision theory: a guide for the Experimentalist, Plenum Press, New York, 1979, Ch. Reactive scattering Cross sections III: quasiclassical and semiclassical methods, p. 505–561.
- [3] L. Bonnet, J. Rayez, Quasiclassical trajectory method for molecular scattering processes: necessity of a weighted binning approach, *Chemical Physics Letters* 277 (1) (1997) 183–190. doi:[https://doi.org/10.1016/S0009-2614\(97\)00881-6](https://doi.org/10.1016/S0009-2614(97)00881-6). URL <https://www.sciencedirect.com/science/article/pii/S0009261497008816>
- [4] J. Ríos, in: An Introduction to Cold and Ultracold Chemistry: Atoms, Molecules, Ions and Rydbergs, Springer International Publishing, 2020, Ch. Cold Chemical Reactions Between Molecular Ions and Neutral Atoms, pp. 215 – 234. [link]. URL <https://books.google.com/books?id=pmcHEAAAQBAJ>
- [5] F. J. Aoiz, V. J. Herrero, V. Sáez Rábanos, Quasiclassical state to state reaction cross sections for $d+h_2(v=0, j=0) \rightarrow hd(v', j') + h$. formation and characteristics of short-lived collision complexes, *The Journal of Chemical Physics* 97 (10) (1992) 7423–7436. arXiv:<https://doi.org/10.1063/1.463514>, doi:10.1063/1.463514. URL <https://doi.org/10.1063/1.463514>
- [6] F. J. Aoiz, L. Bañares, V. J. Herrero, Recent results from quasiclassical trajectory computations of elementary chemical reactions, *J. Chem. Soc., Faraday Trans.* 94 (1998) 2483–2500. doi:10.1039/A803469I. URL <http://dx.doi.org/10.1039/A803469I>
- [7] A. G. S. de Oliveira-Filho, F. R. Ornellas, J. M. Bowman, Quasiclassical trajectory calculations of the rate constant of the $oh + hbr \rightarrow br + h_2o$ reaction using a full-dimensional ab initio potential energy surface over the temperature range 5 to 500 k, *The Journal of Physical Chemistry Letters* 5 (4) (2014) 706–712. doi:10.1021/jz5000325. URL <https://doi.org/10.1021/jz5000325>
- [8] T. Nagy, A. Vikár, G. Lendvay, A general formulation of the quasiclassical trajectory method for reduced-dimensionality reaction dynamics calculations, *Phys. Chem. Chem. Phys.* 20 (2018) 13224–13240.

doi:10.1039/C8CP01600C.

URL <http://dx.doi.org/10.1039/C8CP01600C>

- [9] S. Patra, J. C. San Vicente Veliz, D. Koner, E. J. Bieske, M. Meuwly, Photodissociation dynamics of n_3^+ , *The Journal of Chemical Physics* 156 (12) (2022) 124307. arXiv:<https://doi.org/10.1063/5.0085081>, doi:10.1063/5.0085081.
URL <https://doi.org/10.1063/5.0085081>
- [10] K. Töpfer, M. Upadhyay, M. Meuwly, Quantitative molecular simulations, *Phys. Chem. Chem. Phys.* 24 (2022) 12767–12786. doi:10.1039/D2CP01211A.
URL <http://dx.doi.org/10.1039/D2CP01211A>
- [11] S. Goswami, J. C. San Vicente Veliz, M. Upadhyay, R. J. Bemish, M. Meuwly, Quantum and quasi-classical dynamics of the $c(3p) + o_2(3\sigma_g) \rightarrow co(1\sigma+) + o(1d)$ reaction on its electronic ground state, *Phys. Chem. Chem. Phys.* 24 (2022) 23309–23322. doi:10.1039/D2CP02840A.
URL <http://dx.doi.org/10.1039/D2CP02840A>
- [12] H. Hirzler, J. Pérez-Ríos, Rydberg atom-ion collisions in cold environments, *Phys. Rev. A* 103 (2021) 043323. doi:10.1103/PhysRevA.103.043323.
URL <https://link.aps.org/doi/10.1103/PhysRevA.103.043323>
- [13] J. Pérez-Ríos, Vibrational quenching and reactive processes of weakly bound molecular ions colliding with atoms at cold temperatures, *Phys. Rev. A* 99 (2019) 022707. doi:10.1103/PhysRevA.99.022707.
URL <https://link.aps.org/doi/10.1103/PhysRevA.99.022707>
- [14] H. Hirzler, E. Trimby, R. S. Lous, G. C. Groenenboom, R. Gerritsma, J. Pérez-Ríos, Controlling the nature of a charged impurity in a bath of feshbach dimers, *Phys. Rev. Res.* 2 (2020) 033232. doi:10.1103/PhysRevResearch.2.033232.
URL <https://link.aps.org/doi/10.1103/PhysRevResearch.2.033232>
- [15] V. C. Mota, P. J. S. B. Caridade, A. J. C. Varandas, B. R. L. Galvão, Quasiclassical trajectory study of the $si + sh$ reaction on an accurate double many-body expansion potential energy surface, *The Journal of*

Physical Chemistry A 126 (22) (2022) 3555–3568, pMID: 35612827.
arXiv:<https://doi.org/10.1021/acs.jpca.2c01633>, doi:10.1021/
acs.jpca.2c01633.

URL <https://doi.org/10.1021/acs.jpca.2c01633>

- [16] M. J. Frisch, G. W. Trucks, H. B. Schlegel, G. E. Scuseria, M. A. Robb, J. R. Cheeseman, G. Scalmani, V. Barone, G. A. Petersson, H. Nakatsuji, X. Li, M. Caricato, A. V. Marenich, J. Bloino, B. G. Janesko, R. Gomperts, B. Mennucci, H. P. Hratchian, J. V. Ortiz, A. F. Izmaylov, J. L. Sonnenberg, D. Williams-Young, F. Ding, F. Lipparini, F. Egidi, J. Goings, B. Peng, A. Petrone, T. Henderson, D. Ranasinghe, V. G. Zakrzewski, J. Gao, N. Rega, G. Zheng, W. Liang, M. Hada, M. Ehara, K. Toyota, R. Fukuda, J. Hasegawa, M. Ishida, T. Nakajima, Y. Honda, O. Kitao, H. Nakai, T. Vreven, K. Throssell, J. A. Montgomery, Jr., J. E. Peralta, F. Ogliaro, M. J. Bearpark, J. J. Heyd, E. N. Brothers, K. N. Kudin, V. N. Staroverov, T. A. Keith, R. Kobayashi, J. Normand, K. Raghavachari, A. P. Rendell, J. C. Burant, S. S. Iyengar, J. Tomasi, M. Cossi, J. M. Millam, M. Klene, C. Adamo, R. Cammi, J. W. Ochterski, R. L. Martin, K. Morokuma, O. Farkas, J. B. Foresman, D. J. Fox, Gaussian 16 Revision C.01, gaussian Inc. Wallingford CT (2016).
- [17] W. L. Hase, R. J. Duchovic, X. Hu, A. Komornicki, K. F. Lim, D.-h. Lu, G. H. Peslherbe, K. N. Swamy, S. Linde, A. Varandas, et al., A general chemical dynamics computer program, *Quantum Chem. Program Exch. Bull* 16 (1996) 671.
- [18] C. R. Harris, K. J. Millman, S. J. van der Walt, R. Gommers, P. Virtanen, D. Cournapeau, E. Wieser, J. Taylor, S. Berg, N. J. Smith, R. Kern, M. Picus, S. Hoyer, M. H. van Kerkwijk, M. Brett, A. Haldane, J. F. del Río, M. Wiebe, P. Peterson, P. Gérard-Marchant, K. Sheppard, T. Reddy, W. Weckesser, H. Abbasi, C. Gohlke, T. E. Oliphant, Array programming with NumPy, *Nature* 585 (7825) (2020) 357–362. doi:10.1038/s41586-020-2649-2.
URL <https://doi.org/10.1038/s41586-020-2649-2>
- [19] P. Virtanen, R. Gommers, T. E. Oliphant, M. Haberland, T. Reddy, D. Cournapeau, E. Burovski, P. Peterson, W. Weckesser, J. Bright, S. J. van der Walt, M. Brett, J. Wilson, K. J. Millman, N. Mayorov, A. R. J. Nelson, E. Jones, R. Kern, E. Larson, C. J. Carey, Í. Polat, Y. Feng,

- E. W. Moore, J. VanderPlas, D. Laxalde, J. Perktold, R. Cimrman, I. Henriksen, E. A. Quintero, C. R. Harris, A. M. Archibald, A. H. Ribeiro, F. Pedregosa, P. van Mulbregt, SciPy 1.0 Contributors, SciPy 1.0: Fundamental Algorithms for Scientific Computing in Python, *Nature Methods* 17 (2020) 261–272. doi:10.1038/s41592-019-0686-2.
- [20] J. D. Hunter, Matplotlib: A 2d graphics environment, *Computing in Science & Engineering* 9 (3) (2007) 90–95. doi:10.1109/MCSE.2007.55.
- [21] The pandas development team, pandas-dev/pandas: Pandas (Feb. 2020). doi:10.5281/zenodo.3509134.
URL <https://doi.org/10.5281/zenodo.3509134>
- [22] M. M. McKerns, L. Strand, T. Sullivan, A. Fang, M. A. G. Aivazis, Building a framework for predictive science (2012). arXiv:1202.1056.
- [23] M. McKerns, M. Aivazis, pathos: a framework for heterogeneous computing (2010).
URL <https://uqfoundation.github.io/project/pathos>
- [24] D. T. Colbert, W. H. Miller, A novel discrete variable representation for quantum mechanical reactive scattering via the s-matrix kohn method, *The Journal of Chemical Physics* 96 (3) (1992) 1982–1991. arXiv: <https://doi.org/10.1063/1.462100>, doi:10.1063/1.462100.
URL <https://doi.org/10.1063/1.462100>
- [25] L. Bonnet, The method of gaussian weighted trajectories. iii. an adiabaticity correction proposal, *The Journal of Chemical Physics* 128 (4) (2008) 044109. arXiv:<https://doi.org/10.1063/1.2827134>, doi:10.1063/1.2827134.
URL <https://doi.org/10.1063/1.2827134>
- [26] J. Dormand, P. Prince, A family of embedded runge-kutta formulae, *Journal of Computational and Applied Mathematics* 6 (1) (1980) 19–26. doi:[https://doi.org/10.1016/0771-050X\(80\)90013-3](https://doi.org/10.1016/0771-050X(80)90013-3).
URL <https://www.sciencedirect.com/science/article/pii/0771050X80900133>
- [27] Z.-C. Yan, J. F. Babb, A. Dalgarno, G. W. F. Drake, Variational calculations of dispersion coefficients for interactions among h, he, and li atoms,

- Phys. Rev. A 54 (1996) 2824–2833. doi:10.1103/PhysRevA.54.2824.
URL <https://link.aps.org/doi/10.1103/PhysRevA.54.2824>
- [28] J. Liu, E. J. Salumbides, U. Hollenstein, J. C. J. Koelemeij, K. S. E. Eikema, W. Ubachs, F. Merkt, Determination of the ionization and dissociation energies of the hydrogen molecule, The Journal of Chemical Physics 130 (17) (2009) 174306. arXiv:<https://doi.org/10.1063/1.3120443>, doi:10.1063/1.3120443.
URL <https://doi.org/10.1063/1.3120443>
- [29] A. Shayesteh, S. F. Alavi, M. Rahman, E. Gharib-Nezhad, Ab initio transition dipole moments and potential energy curves for the low-lying electronic states of caH, Chemical Physics Letters 667 (2017) 345–350. doi:<https://doi.org/10.1016/j.cplett.2016.11.020>.
URL <https://www.sciencedirect.com/science/article/pii/S0009261416309022>
- [30] J. Mitroy, J.-Y. Zhang, Properties and long range interactions of the calcium atom, The Journal of Chemical Physics 128 (13) (2008) 134305. arXiv:<https://doi.org/10.1063/1.2841470>, doi:10.1063/1.2841470.
URL <https://doi.org/10.1063/1.2841470>